Supporting Information

Focused ion beam-fabricated high-performance nickel-ruthenium nano-supercapacitor

Sudipta Biswas[a], Ahiud Morag[b,c], Nitzan Shauloff[a], Nitzan Maman[d], and Raz Jelinek[a,d] *
[a.]Department of Chemistry, Ben Gurion University of the Negev, Beer Sheva 8410501, Israel
E-mail: razj@bgu.ac.il
[b.]Center for Advancing Electronics Dresden (CFAED) & Faculty of Chemistry and Food Chemistry, Technische Universität Dresden, Mommsenstrasse 4, Dresden 01069, Germany
[c.]Department of Synthetic Materials and Functional Devices, Max-Planck Institute of Microstructure Physics, Halle 06120, Germany
[d.]Ilse Katz Institute for Nanotechnology, Ben Gurion University of the Negev
Beer Sheva 8410501, Israel

Keywords: focused ion beam; nano-supercapacitors; AC line filters; nickel-ruthenium alloy; ruthenium oxide

Table 1: Comparison of electrochemical parameters in previous reports with the present work

Previous works	Material	Scan rate (V s^{-1})	Performance	Cycling stability (%)	ESR (Ω cm^2)	Year
[25]	$MoTe_2$ (**FIB**)	0.01	7.33 mF cm^{-2}	95	0.035	2015
[26]	MXene/CNT (**FIB**)	0.5	0.035 mF cm^{-2}	80		2021
[35]	Ppy-CNT@rGO	0.1	33 mF cm^{-2}	89.3	.28	2023
[36]	nanoporous gold	1	1.5 mF cm^{-2}	92		2019
[37]	MXene, MWCNT	1	10 mF/cm^{-2}			2019
[38]	organohydrogel	0.2	1.5 mA cm^{-2} (0.15 mF cm^{-2})		0.04	2023
This work	NiRuKI	10	10.5 mF cm^{-2}	94	0.047	
This work	NiRuKI	0.01	28.26 mF cm^{-2}			

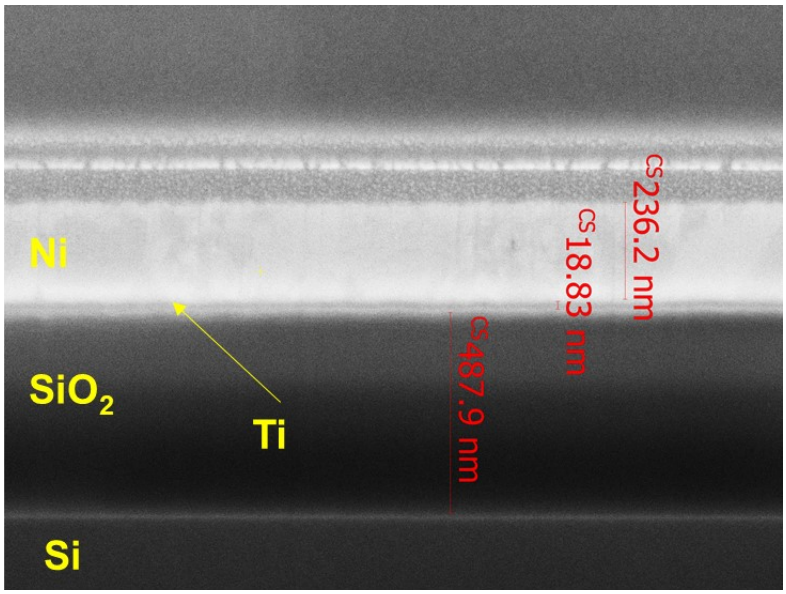

Figure S1. SEM micrograph of cross-sectional view of as fabricated Ni electrode before electrodeposition of NiRu alloy.

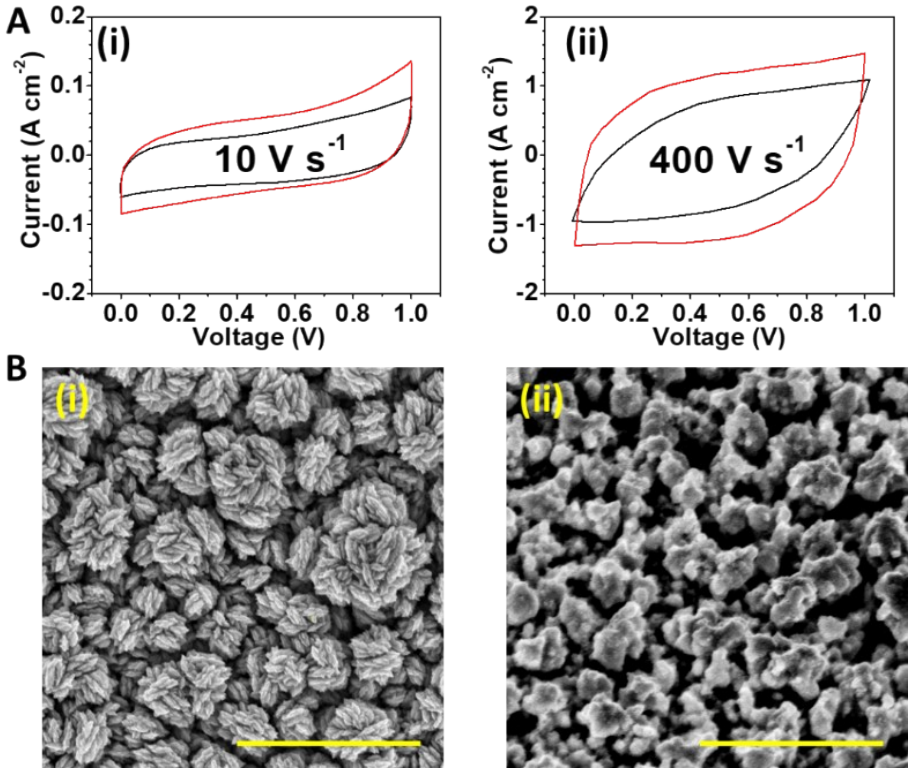

Figure S2. A. CV comparison of the device deposited with (red curve)/without KI (black curve). **B.** SEM showing higher porosity in deposition with KI (ii) compared to deposition without KI (i) (scale-bar corresponds to 1 µm).

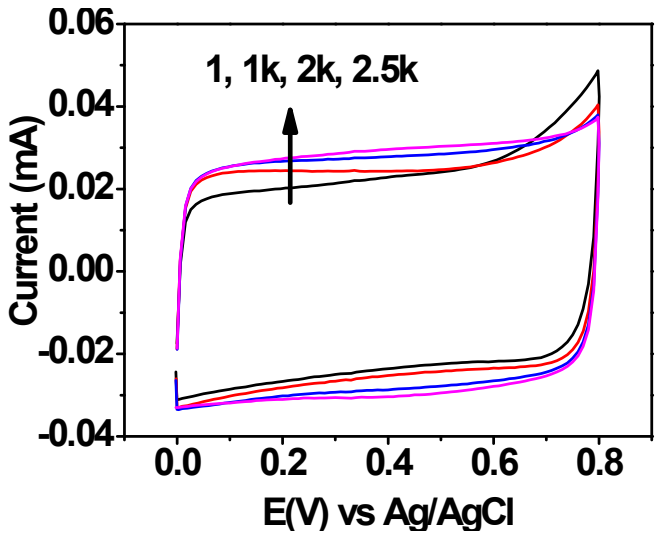

Figure S3: Electrochemical oxidation of Ru. CV curves at different stages of the oxidation showing a mild change of the curve indicating partial oxidation of the Ru. With oxidation CV became more rectangular indication improvement in capacitance.

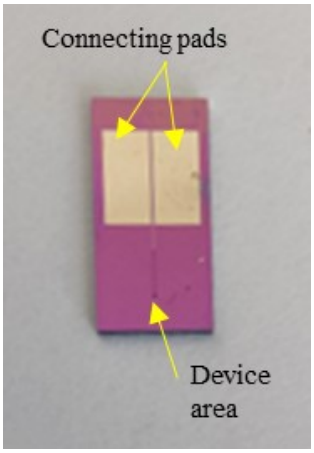

Figure S4: A single device on a silicon wafer where two connecting pads are visible.

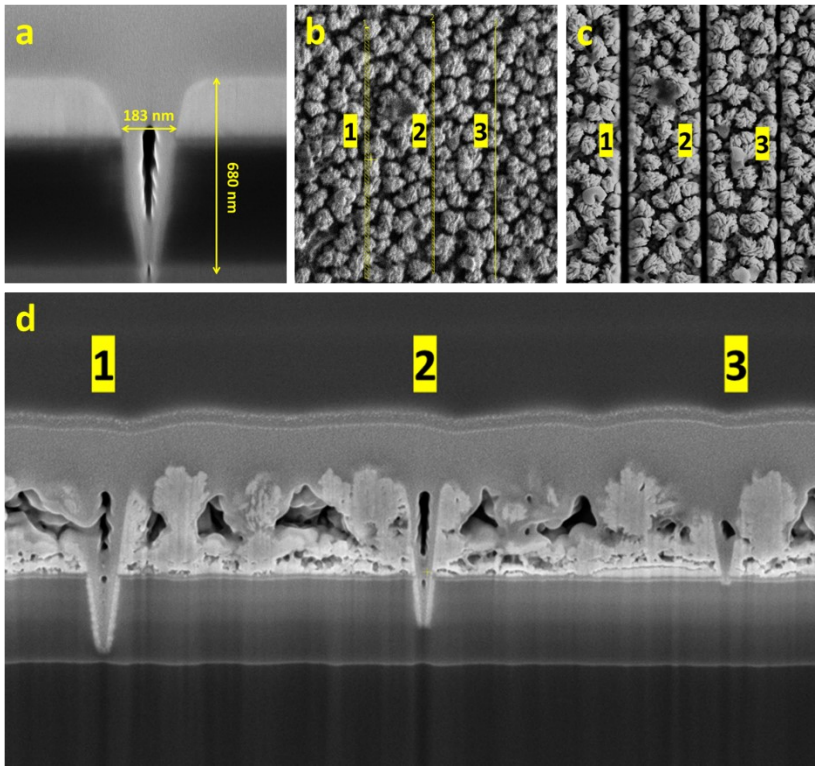

Figure S5: **a.** Vertical cross-section of trench after FIB. **b-c.** Trench 1, 2, 3 created with FIB having varying width with fix FIB operational parameters (viz. beam size, operation current, acceleration voltage, dwell time, etc.). Trench 1, 2 and 3 are created with width 200 nm, 100 nm, 60 nm. This shows when we go for the trench width less 100 nm there is a chance of shorting between the electrode as at 3rd trench, it do not penetrate the nonconducting SiO_2 surface. Also, at this lower trench width some shorting also appeared at top as encircled with yellow circle.

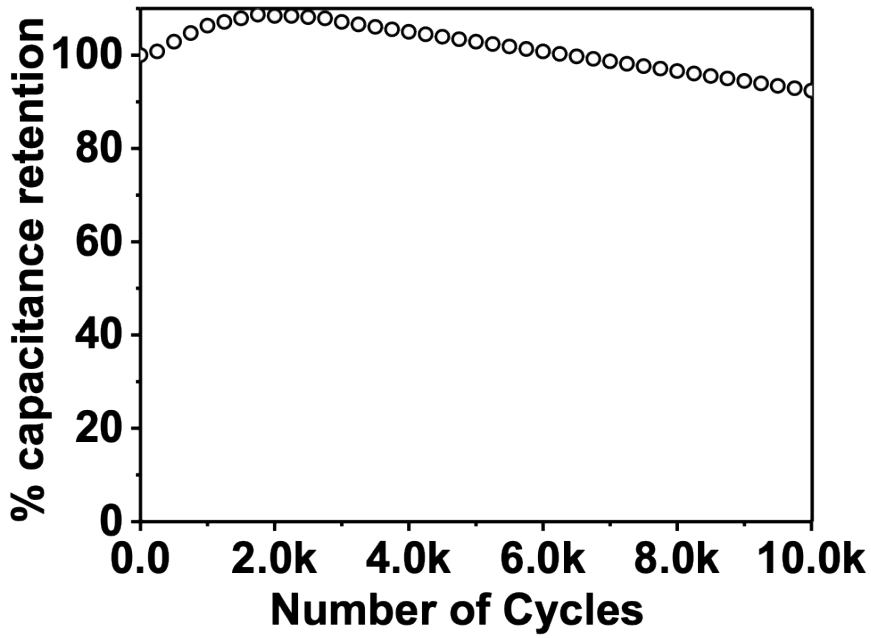

Figure S6: Cycle stability. Capacitance retention as a function of cycle number for NiRu/RuO_2 nano-device using CV measurements at a scan rate of 10 V s^{-1} in a voltage window of 1 V with aqueous electrolyte.